Fast simulation of the CEPC conceptual detector with Delphes and its validation *

Xin. Mo[1)] Gang. Li[1;2)] Manqi. Ruan[1;3)] Xinchou. Lou[1,2)]

[1] Institute of High Energy Physics, Chinese Academy of Sciences, Beijing 100049, China

[2] University of Texas at Dallas, Richardson, TX 75080-3021, USA

Abstract: In this paper, the DELPHES is used to simulate the detector at the Circular Electron-Positron Collider (CEPC). The geometry and performance of the CEPC detector are presented. The fast simulation in the DELPHES framework is validated with a series of benchmark processes, including $e^+e^- \to \mu\mu H$ and H to inclusive decay, $e^+e^- \to q\bar{q}H$ and H to invisible, $e^+e^- \to \nu\bar{\nu}$ and H decaying via double W bosons, and $e^+e^- \to q\bar{q}H,\ H \to q\bar{q}$. The comparisons between DELPHES and the full simulation, which is based on Geant4 & Marlin, shows that DEPHES simulates the CEPC detector well.

Key words: CEPC, DELPHES , Fast simulation

PACS: 13.66.Fg, 14.80.Bn, 07.05.-t

∗ The study was partially supported by the CAS/SAFEA International Partnership Program for Creative Research Teamsand funding from CAS and IHEP for the Thousand Talent and Hundred Talent programs, as well as grants from the State Key Laboratory of Nuclear Electronics and Particle Detectors.

1) E-mail: li.gang@ihep.ac.cn

2) E-mail: manqi.ruan@ihep.ac.cn

1 Introduction

CEPC[1, 2] is a next generation electron-positron collider proposed by Chinese scientists. The machine is expected to collide electron and positron beams at the center-of-mass energy of 240- 250 GeV to maximize the Higgs production cross section of the $e^+e \to ZH$ process, with an instantaneous luminosity of 2×10^{34} cm$^{-2}s^{-1}$. CEPC is designed to deliver a total of 5 ab^{-1} integrated luminosity to two detectors in 10 years, over 10^6 Higgs events will be produced. The large statistics with clean backgrounds will enable CEPC to perform Higgs precision measurements, Standard Model (SM) tests, and searches for potential new physical phenomena. In order to investigate sensitivity to new physics, theorists would get involved and various new models would be tested. To save computing time and to simplify the procedure of full detector simulation and reconstruction, a dedicated fast simulation tool is highly demanded.

DELPHES [3] is a fast simulation framework developed in 2009, and the latest prime version was released in 2013, which is designed for phenomenological studies on the simulation of various detector designs. The DELPHES framework simulates the response of a general purpose collider detector, whose components are organized concentrically with a cylindrical symmetry around the beam axis. The energy and momentum are smeared according to the resolutions of detector. Eventually, all kinds of particles are reconstructed with algorithm based on PFA[4] philosophy, then clustering into jets with FastJet [16] .

This paper is organized as following. In Sect. **2**, the CEPC detector concept are introduced briefly. Then in Sect. **3**, the MC generation, full simulation and reconstruction of detector, and data analysis of e^+e^- experiment are briefly introduced. In Sect. **4**, some benchmark processes are chosen to the validate the simulation of the DELPHES on CEPC by comparing the fast and full simulaitons, including $e^+e^- \to \mu^+\mu^- H$ and Higgs →inclusive, $e^+e^- \to q\bar{q}H$ with Higgs decaying into invisible, $e^+e^- \to \nu\bar{\nu}H$ with Higgs coupling to W boson pair, and $e^+e^{\to} ZH \to 2(q\bar{q})$. In the end the conclusion remarks are presented.

2 CEPC detector conceptual design

The CEPC detector concept design[1] takes the ILC detector, ILD[5, 6], as a reference and adopts the philosophy of PFA, which benefits from a high granularity calorimetric system.

The CEPC detector consists of three main sub-detectors and a superconducting solenoid of 3.5 T. The three sub-detectors are, from inner to outer, a hybrid tracking system composed of several silicon based devices and a

Time Projection Chamber (TPC), a high granularity calorimetry system, and a Muon detector.

The hybrid tracking system has five parts. A vertex detector (VTX), constructed with high spatial pixel sensor, is placed very close to the interaction point (IP) and the inner radius is only 16 mm. The VTX provides very precision measurements of the IP position of tracks and events, which is used for the $b-/c-$jet flavor tagging and τ-tagging. A Silicon Inner Tracker (SIT) is just outside and cooperating with the VTX for vertex reconstruction and flavor tagging. A set of Forward Tracking Disks (FTDs) are placed in the forward region to increase the geometric acceptance of tracking system with coverage up to $|\cos\theta| = 0.99$. A Silicon External Tracker (SET) and End-cap Tracking Disks (ETD) are taken as the outermost layer of whole tracker system, which provide precision position measurements of tracks entering the calorimetric system. The TPC, with a 2.35m half-length and 1.8m outer radius, provides about 200 hits per track and 100μm resolution in $r\phi$ plane, which allow for excellent pattern recognition, track reconstruction efficiency, and potential dE/dx-based particle identification.

A calorimetric system consisting of Electromagnetic Calorimeter (ECAL) and Hadron Calorimeter (HCAL) with very fine granularity is placed inside the solenoid. The system plays an essential role in the Particle-Flow Algorithm (PFA), providing excellent separation of showers from different particles and jet energy resolution of 3-4%.

A superconducting solenoid of 3.5 T is surrounding the calorimetry system. The return yoke is placed outside the solenoid. The CEPC muon system acts as the muon identifier, the solenoid flux return yoke and the support structure for the whole spectrometer. High muon detection efficiency, low hadron mis-identification rate, modest position resolution and large coverage are the main concerns of the design.

3 Monte Carlo samples, detector simulation and reconstruction, and data analysis

For the CEPC detector design and optimization, a whole set of $e^+e^- \to ZH$ signal process and Standard Model (SM) backgrounds have been generated [7] with the generic Monte-Carlo generator Whizard 1.95 [8]. To simulate the detector response, a full simulation package, Mokka [9], based on Geant4 [10] and a fast simulation framework of the Delphes [3] are used. The Particle Flow Algorithm (PFA) philosophy is utilized in the reconstruction of both the full and fast simulation.

After full simulation, hits in different sub-detectors are digitized properly and reconstructed with reconstruction software Marlin [11]. A dedicated PFA, Arbor[12], is used for particle reconstruction, and Pandora [13], an alternative

one, is taken as reference. All jets are reconstructed with LCFIPlus package[14], where a e^+e^- k_t algorithm [15], often referred to also as Durham algorithm, is used for jet-clustering.

The detector model implemented in the DELPHES is same as the one in full simulation but with necessary simplifications. For the charged tracks simulated with DELPHES, there is a common strategy to smear their momentum. The angular resolution is assumed to be perfect, so that the smearing only applied to the transversal momentum. In practice, the resolution of their momentum is described as a Gaussian, which is parameterized function of p_t and η. The values for the simulation is $\sigma = \sqrt{0.001^2 + (10^{-5} p_t)^2}$ as required in CEPC pre-CDR. Then the charged tracks are reconstructed according to the user-defined probability, which are listed in Tab. 1.

Table 1. Efficiencies for charged tracks(%)

	$P_t \leq 0.1$	$P_t > 0.1$
$\eta \leq 3.0$	0	100
$\eta > 3.0$	0	0

For neutral objects which mainly rely on the calorimetric system, some points should be emphasized: 1. The fake rate for electrons, muons and photons is not implemented in the current version of DELPHES ; 2. The photon conversions into electron-positron pairs are ignored neither. Both the true photons and electrons reaching calorimeter without a reconstructed track are considered as photon in DELPHES .

The overall reconstruction of particles implemented in DELPHES is mainly based on a perfect PFA . For the charged tracks, the reconstruction involves both the tracker system and the calorimetric system. Since the resolution of tracking system is better than this of calorimeter in the CEPC energy region, it can be convenient to use the tracking information within the tracker acceptance for estimating the charged particle momenta. The efficiencies could be parameterized as a function of the energy and pseudo-rapidity. For a preliminary study, the present parameters are listed in Tab. 2, which are consistent those of full simulation.

Table 2. Effciencies for identification of γ, $e^{\pm}$, $\mu^{\pm}$

	Energy≤ 2.0	Energy> 2.0
$\lvert\eta\rvert \leq 1.5$	0	0.99
$1.5 < \lvert\eta\rvert \leq 3.0$	0	0.99
$\lvert\eta\rvert > 3.0$	0	0

In Delphes, two sets of 4-vector are provided with PFA, which are named as *particle flow tracks* and *particle flow towers*. For each particle flow object, E_{ECAL}, E_{HCAL} and $E_{ECAL,trk}$, $E_{HCAL,trk}$ are essential for the particle flow reconstruction. E_{ECAL}, E_{HCAL} are the total energy deposited in electromagnetic calorimeter and hadronic calorimeter, $E_{ECAL,trk}$, $E_{HCAL,trk}$ are also the total energy deposited in the calorimeters, but from the charged particle whose track has been reconstructed. Then a quantity E_{tower}^{eflow} is defined as

$$\Delta_{ECAL} = E_{ECAL} - E_{ECAL,trk}, \quad \Delta_{HCAL} = E_{HCAL} - E_{HCAL,trk} \tag{1}$$

$$E_{tower}^{eflow} = \max(0, \Delta_{ECAL}) + \max(0, \Delta_{HCAL}) \tag{2}$$

So for a neutron particle like photon, the particle flow tower can be simply created with the energy E_{ECAL} or E_{HCAL}. Meanwhile, for a charged particle, if $E_{E,HCAL} \leq E_{E,HCAL,trk}$, only a particle flow track will be reconstructed with the energy $E_{E,HCAL,trk}$; if $E_{E,HCAL} > E_{E,HCAL,trk}$, a particle flow track with $E_{E,HCAL,trk}$ and a particle flow tower with E_{tower}^{eflow} will be reconstructed simultaneously.

In order to get same performance of jet-clustering, e^+e^- k_t algorithm is also used for the results of fast simulation. The exclusive mode of fast jet is used and the set of input particles are forced into fixed number of jets without any y_{ij} or P_t cuts, which can be applied at analysis stage.

It is worthy to note that the analysis philosophy at e^+e^- collider is different from the one of hadron colliders, such as the Atlas and the CMS. e^+e^- experiments have much less backgrounds than hadron experiments, and usually almost all final states particles of a event are detected and used in the further analysis. For instance, **all** the final physics objects will be used in the analysis of $e^+e^- \to ZH$, with $Z \to \mu^+\mu^-$ and $H \to 2$Jets. In the event selection, the muon pair should be identified firstly with both Pid and kinematic constrains. And then, the remain particles are forced into 2 jets with exclusive mode of $ee-kt$ jet-clustering algorithm, whose y_{ij} will be used to suppress the combinatorial and other backgrounds in the further analysis procedure.

4 Validation with full simulation

The simulation and reconstruction in DELPHES must be validated by comparing the resolutions of all output objects to those of full simulation, as well as the efficiencies. Several benchmark processes are selected, which cover all the physics objects of CEPC experiments, such as tracks, photons, and jets.

4.1 $e^+e^- \to \mu^+\mu^- H$

For $\mu^+\mu^- H$ channel, the di-muons come from Z boson decay, and Higgs is tagged from the recoiling side, so the invariant mass of those systems represent Z meanwhile the recoiling mass is Higgs. Fig. 1 and Fig. 2 show the comparisons of invariant mass of and recoil mass against $\mu^+\mu^-$ pair.

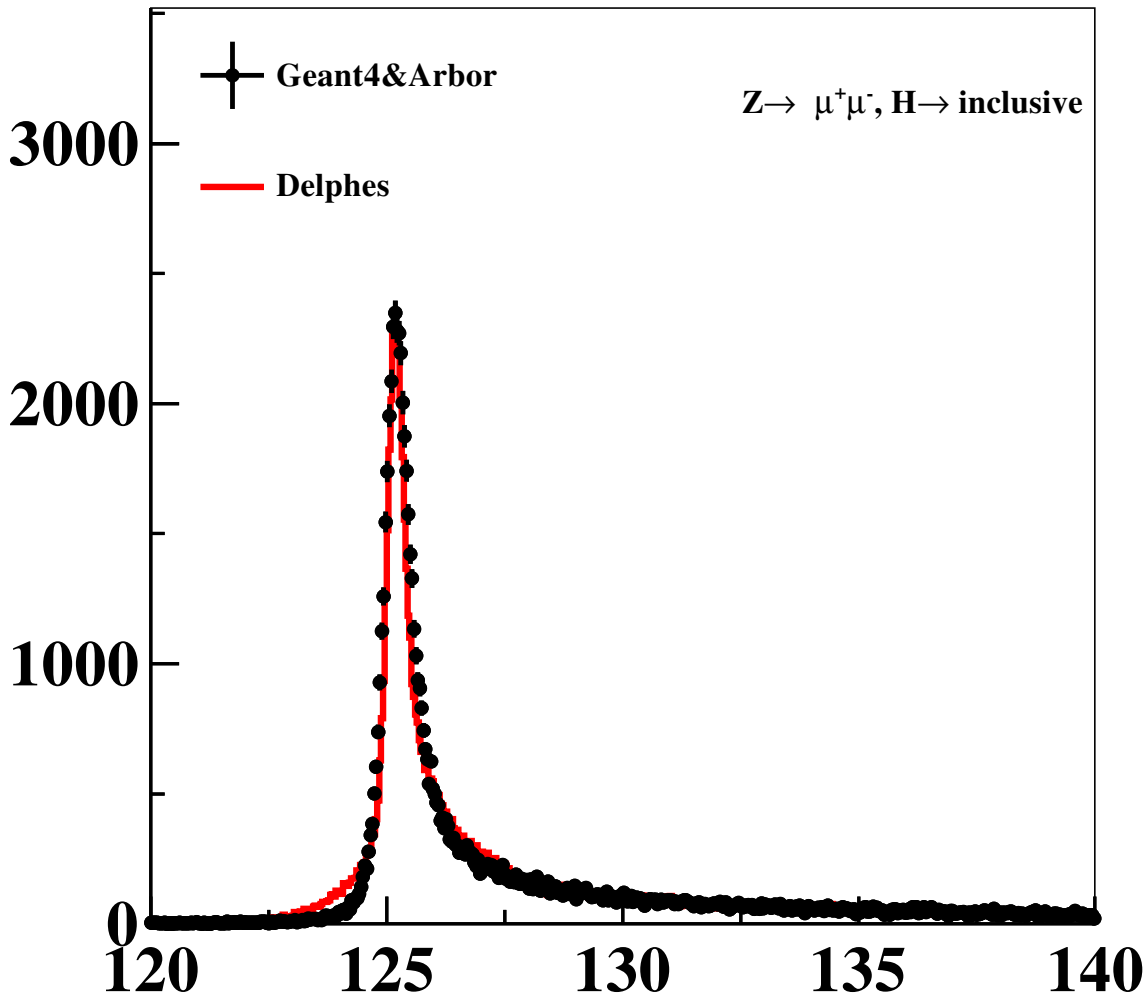

Fig. 1. Recoiling mass against $\mu^+\mu^-$.

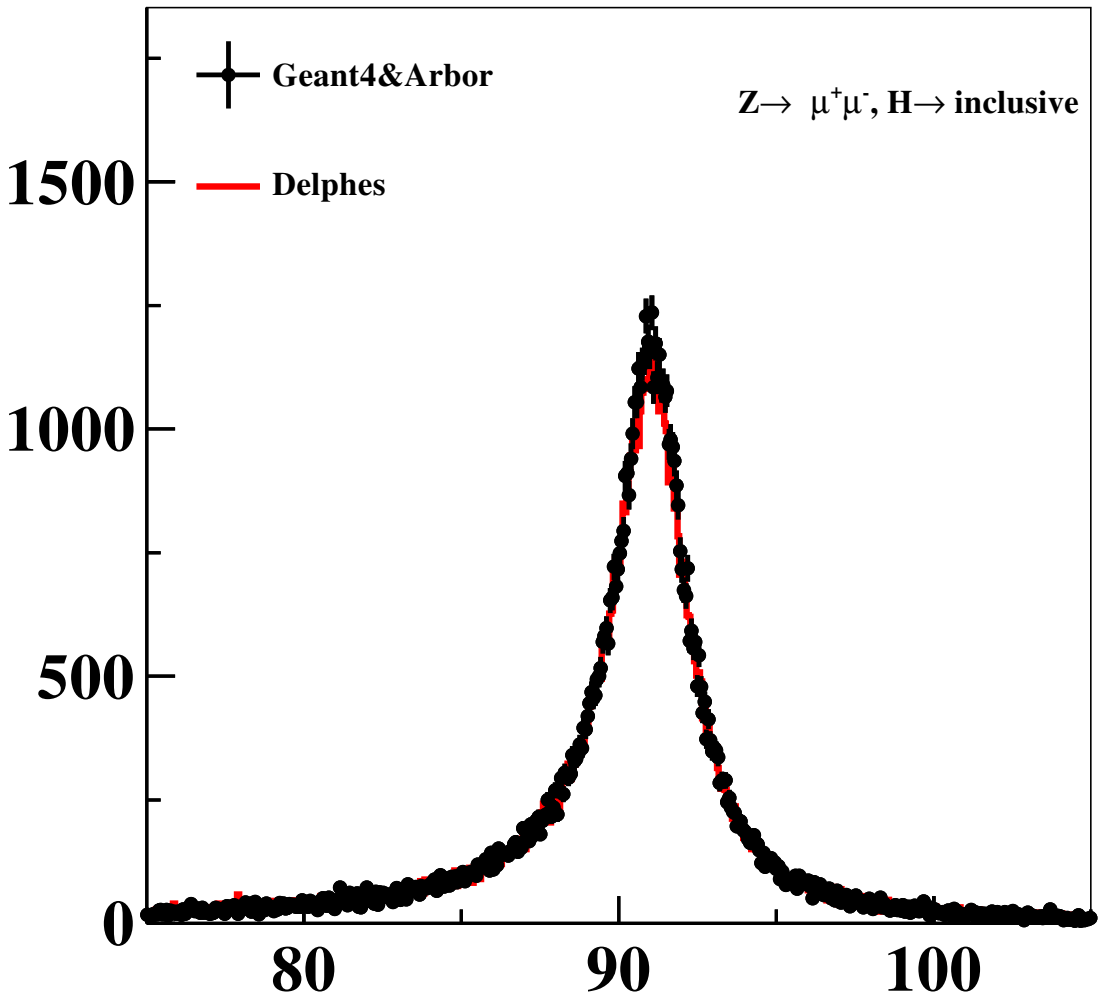

Fig. 2. Invariant mass of $\mu^+\mu^-$.

4.2 $e^+e^- \to q\bar{q}H,\ H \to$ invisible and $e^+e^- \to \nu\bar{\nu}H, H \to q\bar{q}$

There are only two jets in the $e^+e^- \to q\bar{q}H$, $H \to$ invisible and $e^+e^- \to \nu\bar{\nu}H, H \to q\bar{q}$ processes, which can be used to check the performance of jet-clustering and jet energy resolution. The Z mass in $q\bar{q}H$ channel is rescaled after Arbor's output, the final effect of the rescaling is a translation from right to left in X-axis. This operation could be considered as an calibration for the reconstruction scheme.

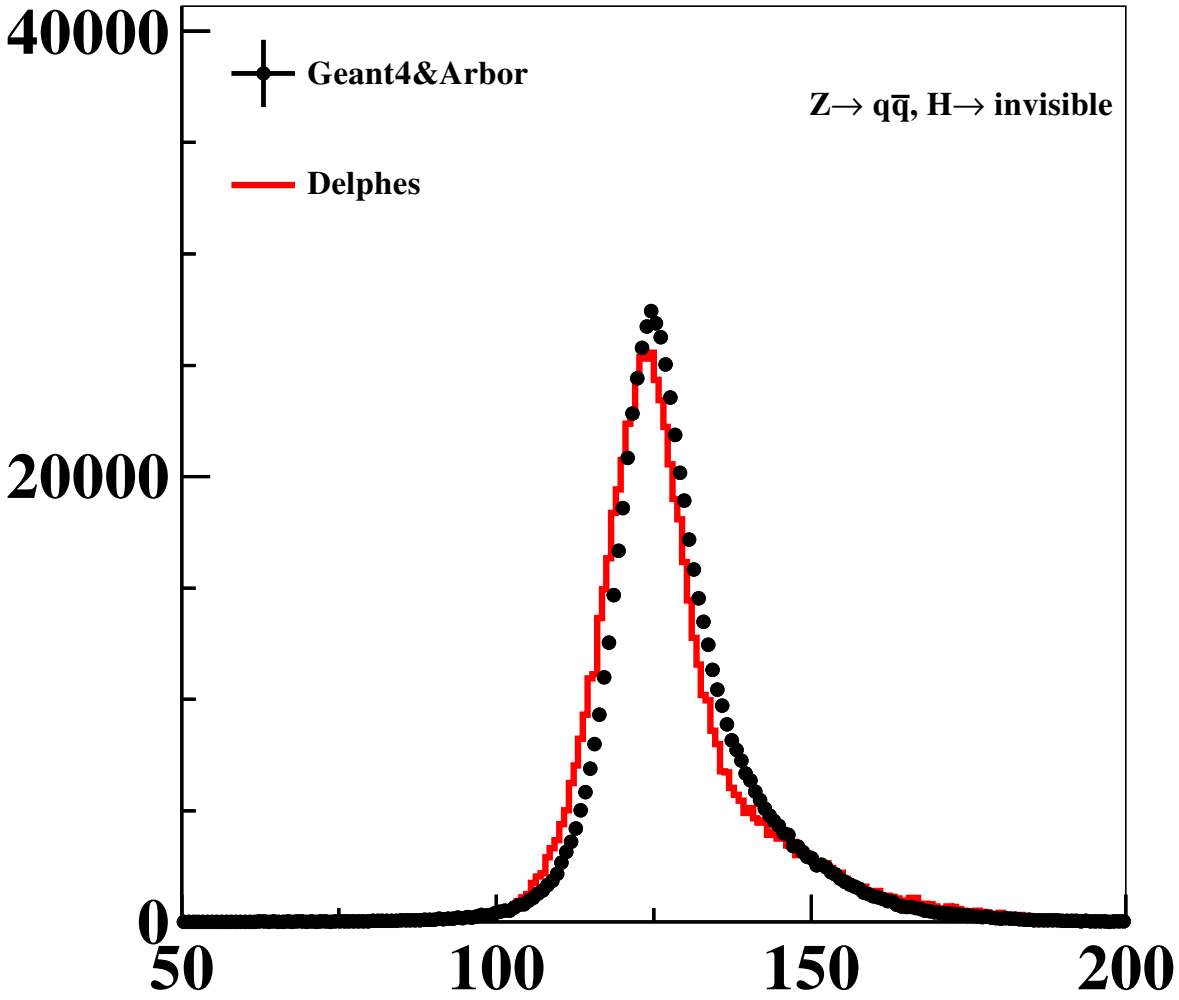

Fig. 3. Recoiling mass against $q\bar{q}$.

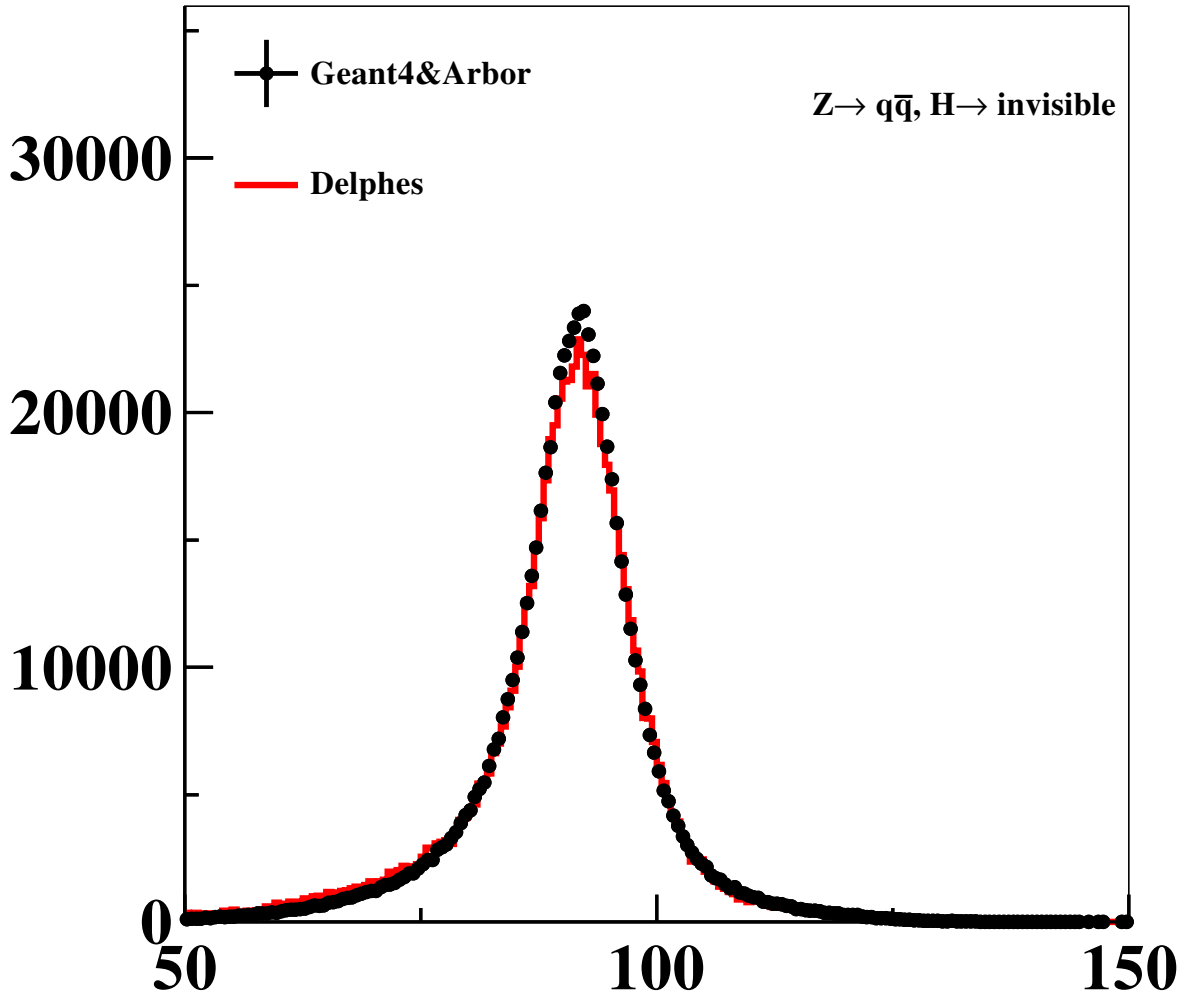

Fig. 4. Invariant mass of $q\bar{q}$.

4.3 $e^+e^- \to \nu\bar{\nu}H,\ H \to WW^*$

In $e^+e^- \to \nu\bar{\nu}H,\ H \to WW^*$, all the visible information comes from WW^* and eventually from Higgs, so in Fig. 6 and Fig. 5 the invariant mass represent Higgs and recoiling side is Z.

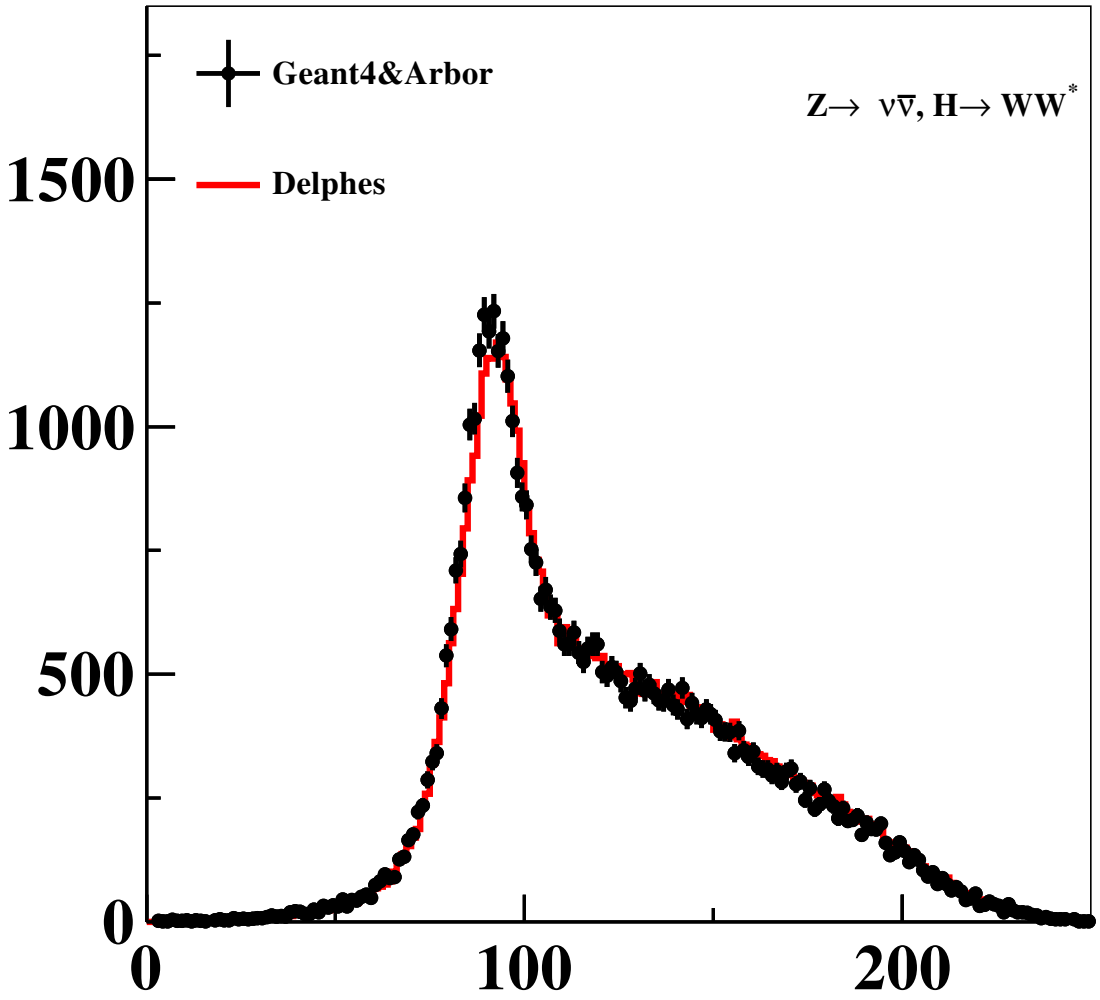

Fig. 5. Recoiling mass against WW^* in $n\bar{n}h \to WW^*$.

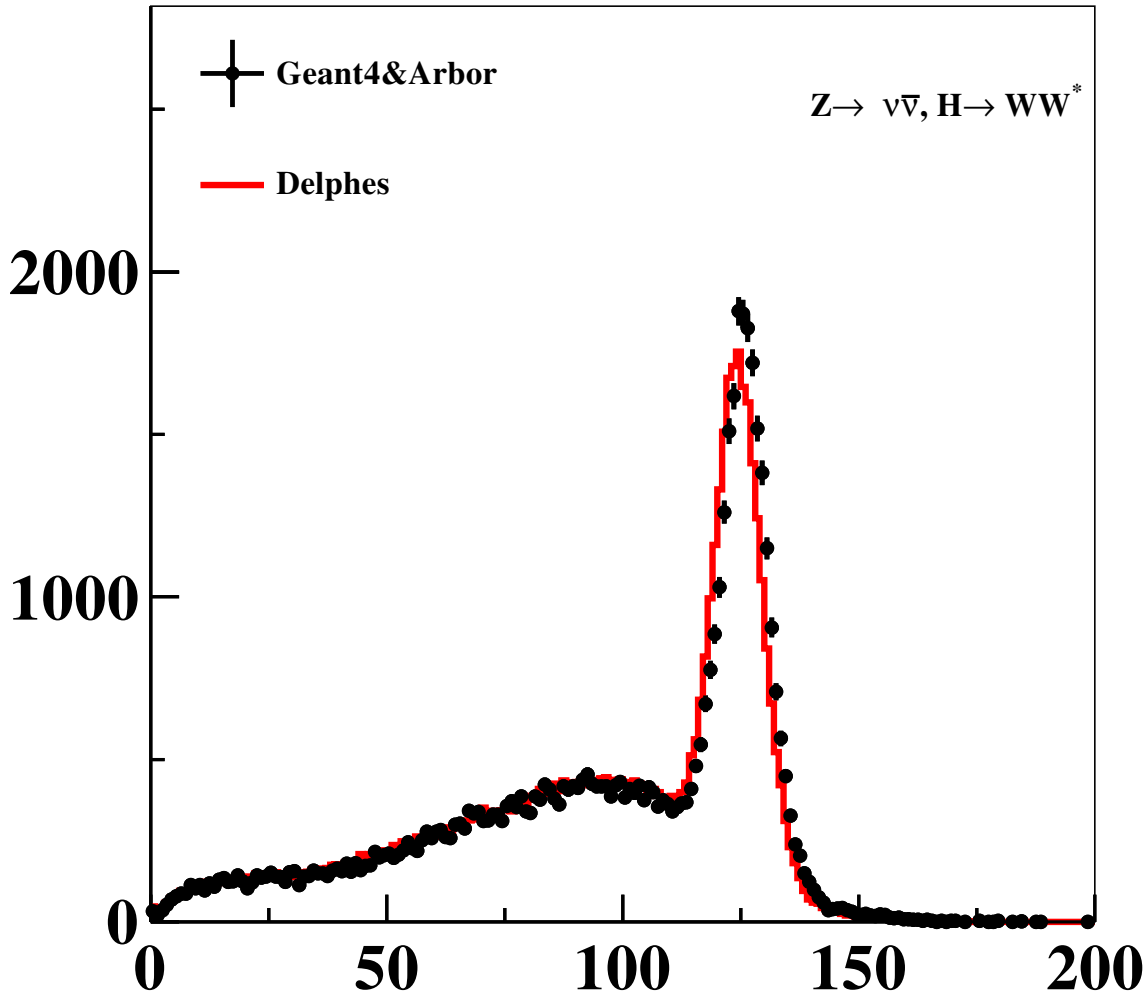

126

Fig. 6. Visible mass in $n\bar{n}h \to WW^*$.

4.4 $e^+e^- \to ZH \to 2(q\bar{q})$

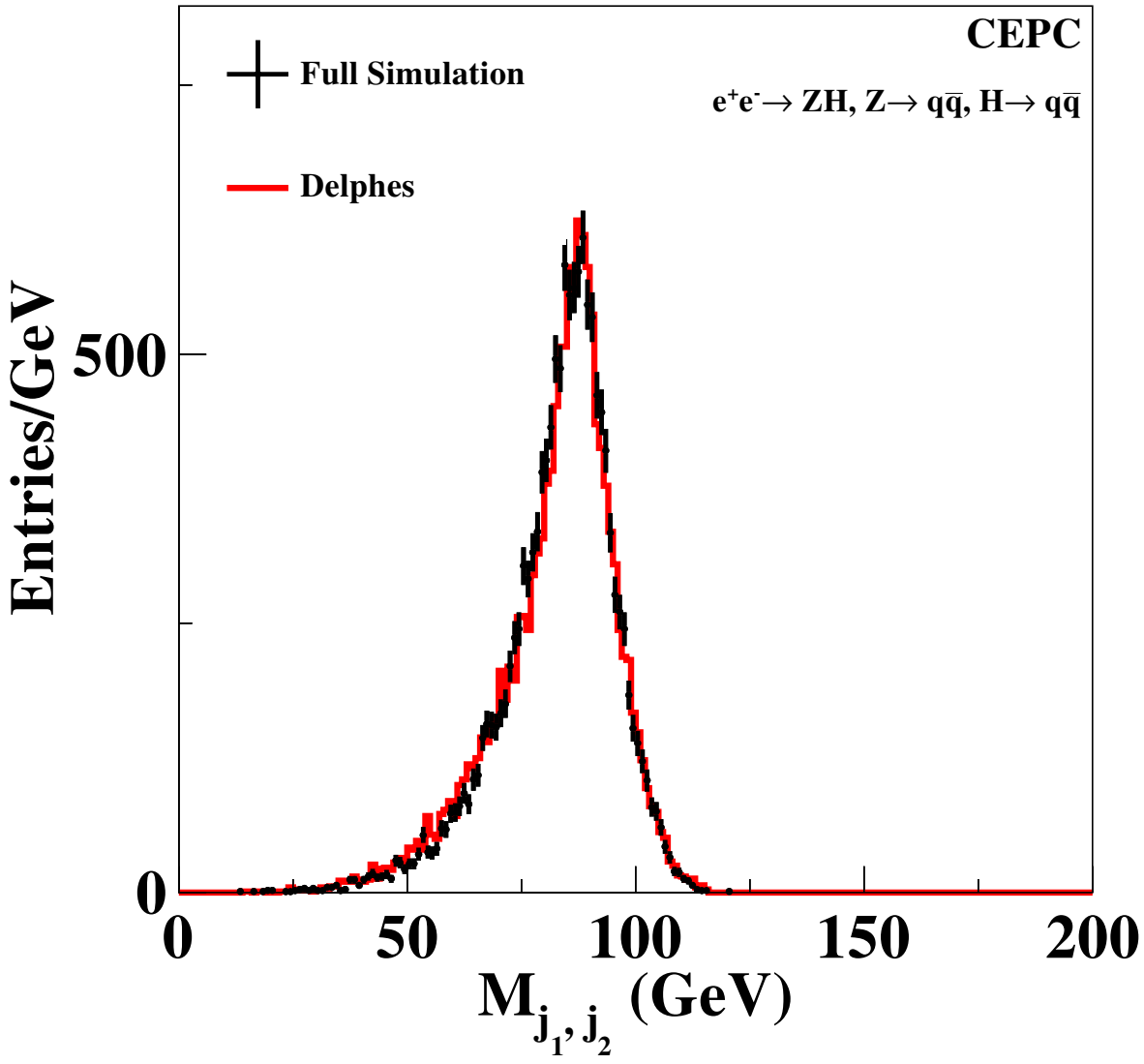

Fig. 7. Invariant mas of jet pair, peaking at Z mass.

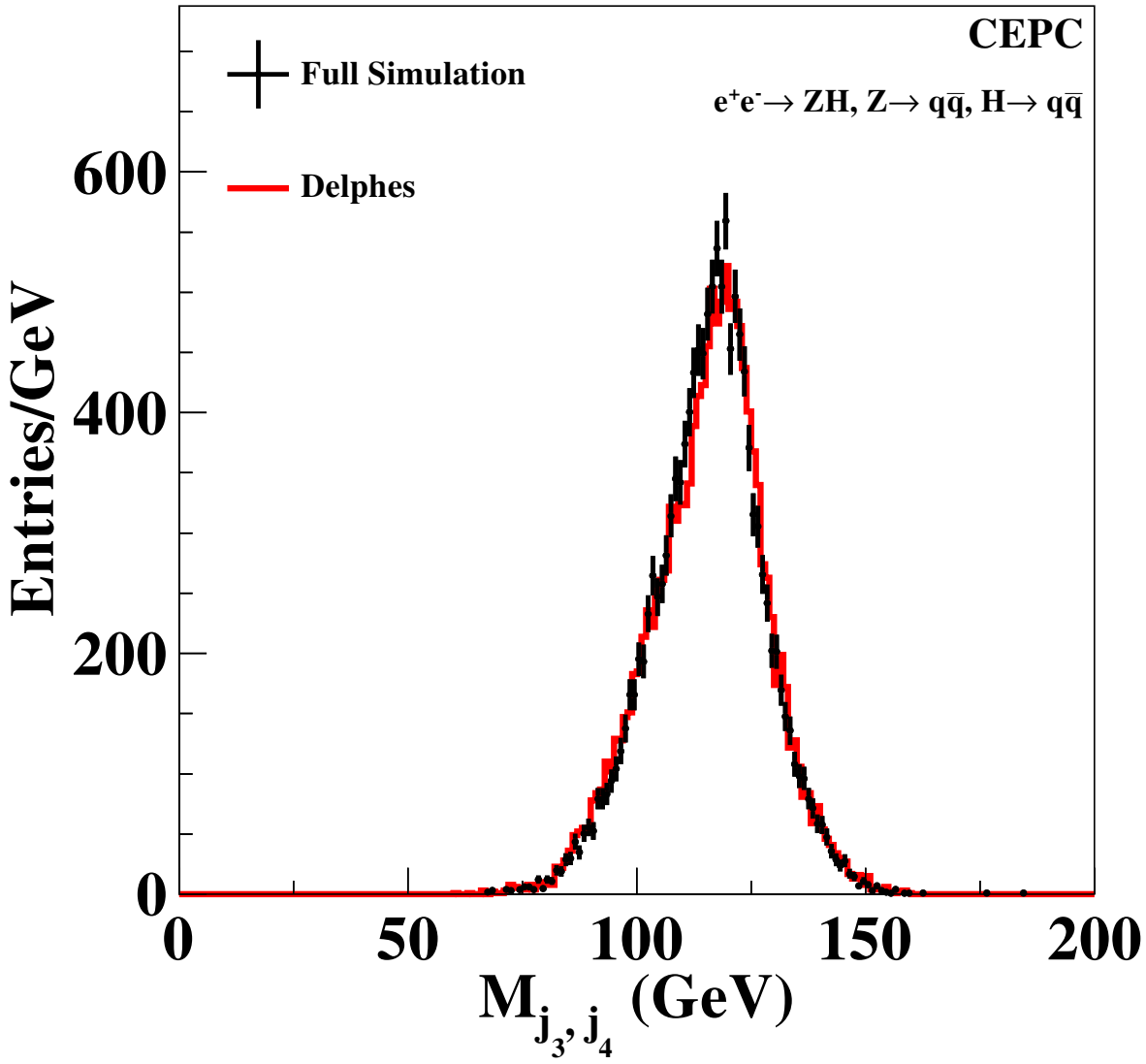

Fig. 8. Invariant mas of jet pair, peaking at Higgs mass

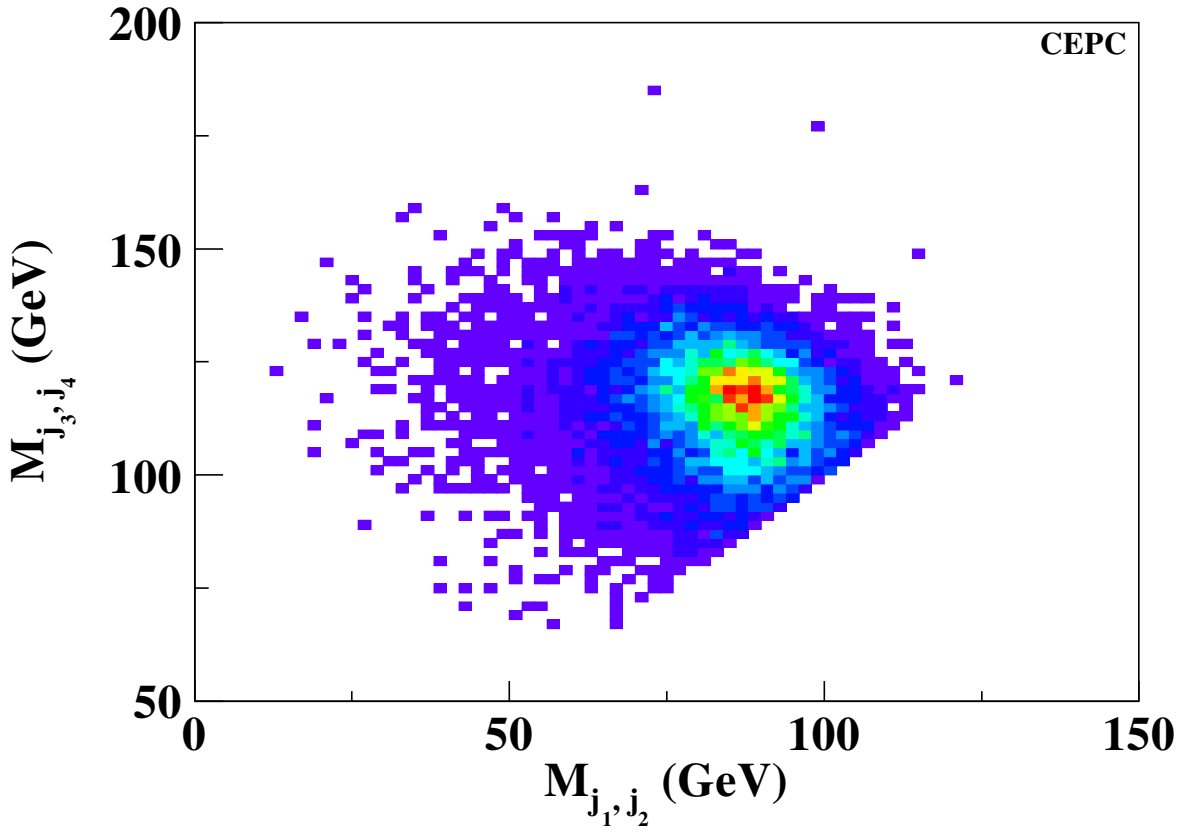

Fig. 9. Scattering plot of M_{j_1,j_2} vs. M_{j_3,j_4} for full simulation

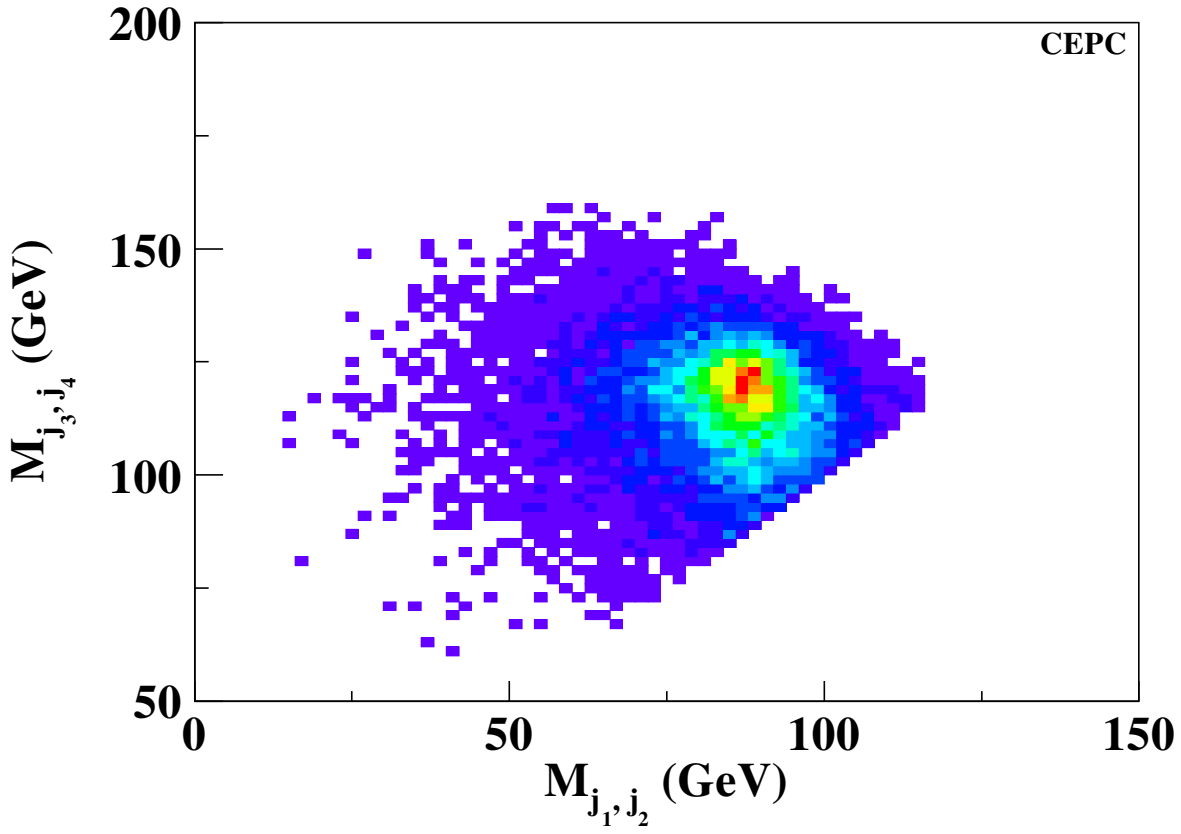

Fig. 10. Scattering plot of M_{j_1,j_2} vs. M_{j_3,j_4} for fast simulation

5 Conclusion

To validate the flexibility of DELPHES on CEPC, a comparison between DELPHES simulation and Geant4 & Arbor has been studied in this paper. In the current study, the results agree very well with our previous understanding for full simulation of CEPC. It should be noted that the DELPHES parametrization has not been all covered in this study, such as those related to flavor tagging. Meanwhile, most of the parameters have to be determined with the feedback from the full simulation.

References

1 CEPC-SppC Preliminary Conceptual Design Report: Physics and Detector, by the CEPC Study Group.

2 CEPC Accelerator Preliminary Conceptual Design Report, by the CEPC Study Group.

3 S. Ovyn, X. Rouby, V. Lemaitre, DELPHES , a framework for fast simulation of a generic collider experiment, arXiv:0903.2225 [hep-ph].

4 P. Janot, Particle Flow Event Reconstruction from LEP to LHC, Presented at Excellence in Detectors and Instrumentation Tech-

nologies workshop, CERN, 2011.

5 T. Abe et al., The International Large Detector: Letter of Intent, arXiv:1006.3396 [hep-ex].

6 T. Behnke et al., The International Linear Collider Technical Design Report - Volume4:Detectors,arXiv:1306.6329 [physics.ins-det].

7 X. Mo, G. Li, M. Ruan, X. Lou, Physics cross sections and event generation of $e^+e^?$ annihilations at the CEPC, Chi. Phys. C, 2016, **40**: 033001.

8 W. Kilian, T. Ohl, J. Reuter, Eur. Phys. J. C, 2011, **71**:1742.

9 P. Mora de Freitas and H. Videau, LC-TOOL-2003-010.

10 S. Agostinelli et al., GEANT4: A simulation toolkit, Nucl. Instrum. Meth. A, 2003, **506**:250.

11 http://ilcsoft.desy.de/portal/software_packages/marlin/index_eng.html

12 M. Ruan, H. Videau, Arbor, a new approach of the Particle Flow Algorithm, arXiv:1403.4784 [physics.ins-det]

13 M. A. Thomson, Nucl. Instrum. Meth. A **611**, 25 (2009) doi:10.1016/j.nima.2009.09.009 [arXiv:0907.3577 [physics.ins-det]].

14 T. Suehara and T. Tanabe, Nucl. Instrum. Meth. A **808**, 109 (2016) doi:10.1016/j.nima.2015.11.054 [arXiv:1506.08371 [physics.ins-det]].

15 S. Catani, Y. L. Dokshitzer, M. Olsson, G. Turnock and B. R. Webber, Phys. Lett. B **269**, 432 (1991);

16 M. Cacciari, G. P. Salam, Phys. Lett. B, 2006, **641**:57 [hep-ph/0512210], M. Cacciari, G.P. Salam, G. Soyez, Eur. Phys. J. C, 2012, **72**:1896[arXiv:1111.6097].

17 F. Gaede, T. Behnke, N. Graf, T. Johnson, arXiv:physics/0306114.